Coverage and Capacity in mmWave Cellular Systems

Salam Akoum, Omar El Ayach, and Robert W. Heath, Jr.
Wireless Networking and Communication Group
The University of Texas at Austin
2501 Speedway Stop, C0806, Austin, TX 78712-0240
{salam.akoum, omarayach, rheath}@mail.utexas.edu

***Abstract*—Millimeter wave (mmWave) communication has recently been proposed for use in commercial cellular systems as a solution to the microwave spectrum gridlock. MmWave spectrum is (potentially) available around the globe and recent hardware advances make mass market deployments feasible. In this paper, we study the coverage and capacity of mmWave cellular systems with a special focus on their key differentiating factors such as the limited scattering nature of mmWave channels, and the use of RF beamforming strategies such as beam steering to provide highly directional transmission with limited hardware complexity. We show that, in general, coverage in mmWave systems can rival or even exceed coverage in microwave systems assuming that the link budgets promised by existing mmWave system designs are in fact achieved. This comparable coverage translates into a superior average rate performance for mmWave systems as a result of the larger bandwidth available for transmission.**

I. Introduction

Physical layer enhancements, such as orthogonal frequency division multiplexing, multiple antennas, and efficient channel coding, have all been successful in increasing spectral efficiency (bits/sec/Hz) in cellular systems [1]. Heterogeneous networks and small cells promise to further increase *area spectral efficiency* (bits/s/Hz/km^2) [2]. As the demand for mobile data continues to grow, however, the microwave spectrum hosting the overwhelming majority of commercial access technologies has become crowded. Exploiting other spectrum bands may help in resolving the current spectrum gridlock. Millimeter (mmWave) communication, for example, has enabled gigabit-per-second data rates in both indoor [3], and fixed outdoor systems. Recent advances in mmWave hardware [4], and the availability of mmWave spectrum, however, has spurred industry interest in leveraging mmWave for outdoor cellular deployments [5].

Initial work on mmWave cellular systems is promising [4]–[11]. Propagation studies in the 38 GHz band indicate that mmWave channels may be more conducive to cellular communication than previously imagined [6], [7]. Key propagation quantities, such as the pathloss exponent, were found to be similar to those experienced in microwave cellular systems [6]. Further, measurements characterizing the scattering in mmWave channels indicate that non-line-of-sight communication is possible if enough array gain is achieved through beamforming [6], [7]. Simultaneously, progress on antenna array design has demonstrated the feasibility of packing large steerable arrays in small form factors [4], [8], [9]. Thus, practical mmWave hardware [4] and existing beamforming solutions [10]–[13],can provide the array gain needed to overcome the increased pathloss at higher frequencies as well as the adaptive beamforming capability needed to ensure proper coverage in random fading environments. While these results demonstrate favorable link-level performance, much less is known about mmWave network performance. System level results are limited to the numerical results in [8] and the medium access control analysis in [14].

In this paper we analyze the performance of mmWave cellular systems. We assume the transmitters and receivers are randomly distributed according to a spatial point process. Random spatial models for base station locations have been shown to be both accurate and tractable in analyzing the performance of cellular networks [15]. In this paper, we incorporate mmWave's key differentiating factors such as (i) the increased reliance on line-of-sight transmission, (ii) the limited scattering in mmWave channels, and (iii) the effect of highly directional transmission. We compare the coverage achieved by mmWave cellular systems to that achieved in standard microwave cellular systems. Microwave cellular systems are assumed to serve single users via simple dominant eigenmode beamforming, or serve multiple users via zero-forcing precoding. Since mmWave hardware constraints preclude such digital precoding, mmWave base stations are assumed to serve users by simply steering their array responses toward the users in their own cell. We characterize analytically coverage in terms of key system parameters such as, signal-to-interference-plus-noise ratio (SINR), base station density, number of users per cell, and various antenna array parameters such as half-power beamwidth. We show that, in general, coverage in mmWave systems can rival or even exceed coverage in microwave systems provided that a sufficient link budget, as given in [5], [8], can be maintained.

The authors at The University of Texas at Austin were supported in part by a gift from Huawei Technologies and the Army Research Laboratory contract: W911NF-10-1-0420.

II. System Description and Assumptions

In this section, we present the random spatial model for the transmitters and receivers, and introduce the system models considered for microwave and mmWave cellular systems.

A. Network Model

Consider a cellular model where the base stations are represented by an independent two-dimensional homogeneous Poisson point process (PPP) [15]. The users are located according to an independent stationary point process. The cells of the base stations form a Voronoi tessellation of the plane with respect to the point process, and the users are connected to their closest base station. We denote the mmWave base station location process by Φ_{mw} of density λ_{mw} base stations per unit area. Similarly, the microwave base station location process is denoted by $\Phi_{\mu\mathrm{w}}$ with density $\lambda_{\mu\mathrm{w}}$ base stations per unit area. The densities of the mmWave and microwave cellular systems need not be the same. It is suggested that mmWave networks are to be denser than microwave networks [5].

We assume that all base stations are active during each transmission, and that each base station serves the same number of active users per cell. By the stationarity of the Poisson process, we consider the performance of a typical base station-user link, denoted by b_0-u_0. By Slivnyak's theorem [16], the process of base stations causing interference to the typical user u_0 form a homogeneous PPP of density λ_{mw} in the case of mmWave systems, and $\lambda_{\mu\mathrm{w}}$ in the case of microwave systems.

B. Microwave System Model

We assume that each base station is equipped with N_{t} antennas, and serves users equipped with single antennas. Each base station can serve $K \leq N_{\mathrm{t}}$ users simultaneously using zero-forcing precoding, and equal power allocation is assumed. The symbol transmitted by the ℓ-th base station to the k-th user is denoted by $s_{\ell,k}$, such that $\mathbb{E}[|s_{\ell,k}|^2] = \frac{1}{K}$. The direct narrowband channel between b_0 and u_0 is denoted by $\mathbf{h}_0^* \in \mathbb{C}^{1\times N_{\mathrm{t}}}$. The interfering channel from the ℓ-th base station to u_0 is denoted by $\mathbf{g}_{0,\ell}^* \in \mathbb{C}^{1\times N_{\mathrm{t}}}$. The direct and interfering channels are assumed to be Rayleigh fading, i.e, each channel entry is an i.i.d. zero mean unit variance complex Gaussian. All base stations are assumed to transmit with power $P_{\mathrm{t},\mu\mathrm{w}}$. The average received signal power from base station b_ℓ at user u_0 is given by $\gamma_{0,\ell} = \frac{P_{\mathrm{t},\mu\mathrm{w}}}{\mathrm{PL}_{\mathrm{ref}}}\left(\frac{d_\ell}{d_{\mathrm{ref}}}\right)^{-n}$, where $\mathrm{PL}_{\mathrm{ref}}$ is the pathloss at a reference distance d_{ref}. We note that $\mathrm{PL}_{\mathrm{ref}}$ is a function of the carrier frequency. The distance d_ℓ is the distance from b_ℓ to u_0 such that $d_\ell > d_0\ \forall \ell \neq 0$, and n is the pathloss exponent. The baseband discrete-time input-output relation for u_0 is given by

$$y_0 = \sqrt{\gamma_0}\mathbf{h}_0^*\mathbf{f}_0 s_0 + \sum_{b_\ell \in \Pi_b / b_0} \sqrt{\gamma_{0,\ell}}\mathbf{g}_{0,\ell}^*\mathbf{F}_\ell \mathbf{s}_\ell + v_0 \qquad (1)$$

where y_0 is the received signal at u_0, the vector $\mathbf{f}_0 \in \mathbb{C}^{N_{\mathrm{t}}\times 1}$ is the unit-norm beamforming vector used by b_0 to transmit u_0's message, and $\mathbf{F}_\ell \in \mathbb{C}^{N_{\mathrm{t}}\times K}$ is the zero-forcing precoder used by the ℓ-th base station. Note that due to the use of zero-forcing precoding, (1) contains no intra-cell interference terms. The scalar v_0 denotes the additive white Gaussian noise with variance σ^2 observed by the receiver.

C. Millimeter Wave System Model

Millimeter wave systems will use large arrays at the transmitter and receiver to obtain enough array gain to provide high data rate communication. Due to circuit design constraints, mmWave systems in the near-term will likely employ analog beamforming, as opposed to digital. In this paper, we assume that directional beamforming is employed. When using beam steering, directionality can be accounted by considering the antenna array's beam pattern which gives the power gain as a function of the elevation and the azimuth angle coordinates. In this paper, we consider linear antenna arrays and thus do not consider beamforming in the elevation domain.

We adopt an idealized yet tractable piecewise-linear array pattern that is a good approximation for practical radiation patterns [17]. Assuming broadside transmission, i.e., maximum gain at an azimuth angle of 0, the *normalized* array gain $\bar{\alpha}^2(\theta)$ at an azimuth angle θ is given by

$$\bar{\alpha}^2(\theta) = \begin{cases} 1 & \text{for } |\theta| < \theta_1 \\ \left|1 - \frac{|\theta|-\theta_1}{2(\theta_{3\mathrm{dB}}-\theta_1)}\right| & \text{for } \theta_1 < |\theta| \leq \theta_2 \\ \mathrm{FBR} & \text{for } \theta_2 < |\theta| \leq \pi \end{cases} \qquad (2)$$

where FBR denotes the front-to-back ratio. The half-power beamwidth is denoted by $\theta_{3\mathrm{dB}}$. The variables $\theta_{3\mathrm{dB}}, \theta_1, \theta_2$ together control the array manifold shape, the half-power bandwidth, and the front-to-back ratio. When beam steering is used to move the location of the beam center from broadside, $\theta = 0$, to some other look direction θ_{center}, the array pattern in (2) holds by simply replacing or reinterpreting $\bar{\alpha}^2(\theta)$ as $\bar{\alpha}^2(\theta - \theta_{\mathrm{center}})$. The radiation pattern is used as a mark for the Poisson point process and all transmitters are assumed to have the same radiation pattern shape.

Scattering in mmWave channels is expected to be sparse and only a few propagation paths are likely to exist between transmitter and receiver [7]. Beam steering is thus used by a transmitter to direct signals in the direction of the most dominant physical path to its receiver. We denote the scalar channel gain of the path between base station b_0 and user u_0 selected via beam steering as h_0. We assume h_0 is Nakagami-m_0 distributed to account for the possible line-of-sight component in the channel and to model the improved fading distribution as a result of beam steering or path selection. The interfering channels, however, are assumed to be Rayleigh-distributed, since the paths on which the interference is received at u_0 are not considered in the

beam steering decisions and are thus assumed to have a less reliable fading distribution.

For multi-user beamsteering, we assume that each base station selects K users to serve and with the help of K transmit chains is able to steer a beam toward each of these users. We do not consider user scheduling, and thus account for intra-cell interference resulting from overlapping beams at the base station. The interference to user u_0 resulting from b_0's transmissions to other users in the same cell are observed through the scalar channels $h_{0,k}$ $\forall k = 1, \ldots, K-1$. The interfering channels from the ℓ-th base station to u_0 are denoted by $g_{\ell,k}$ $\forall$ $k = 0, \ldots, K-1$. The received signal powers from base station b_ℓ at u_0 are denoted by $\gamma_{0,\ell} = \frac{P_{\mathrm{t,mw}}}{PL_{\mathrm{ref}}}\left(\frac{d_\ell}{d_{\mathrm{ref}}}\right)^{-n}$, where $P_{\mathrm{t,mw}}$ denotes the transmit power at the mmWave base stations. This model does not include the effects of signal blockage and penetration losses that can be accounted for by considering the random shape model in [18]. Note that for mmWave transmissions, the log-distance dependent component $\gamma_{0,\ell}$ is expected to be comparable to its microwave counterpart, due to the larger array gains that help offset the larger losses at mmWave frequencies [5]. The received signal at u_0 is

$$y_0 = \sqrt{\gamma_0}\bar{\alpha}(0)h_0 s_0 + \underbrace{\sqrt{\gamma_0}\sum_{k=1}^{K-1}\bar{\alpha}(\theta_{0,k})h_{0,k}s_{0,k}}_{\text{intra-cell interference}} + \underbrace{\sum_{b_\ell\in\Pi_b/b_0}\sqrt{\gamma_\ell}\sum_{k=0}^{K-1}g_{\ell,k}\bar{\alpha}(\theta_{\ell,k})s_{\ell,k}}_{\text{inter-cell interference}} + v_0, \tag{3}$$

where we recall that $\bar{\alpha}(0) = 1$ is the normalized beam pattern from b_0 to u_0 assuming perfect beamsteering toward the desired user. The variables $\theta_{\ell,k}$ $\forall \ell, k$ represent the azimuth angles of the intra-cell and inter-cell interfering paths between base station b_ℓ and user u_0 relative to the beam steering angle used by b_ℓ to transmit data to its k-th user. Intra-cell interference can be reduced by better beamforming or by selecting users whose desired and interfering beams do not significantly overlap.

III. Performance Analysis for Single User Systems

When each base station serves a single user per cell, inter-cell interference is the only source of interference. The received signal at the typical user u_0 for mmWave transmission is given by

$$y_0 = \sqrt{\gamma_0}\bar{\alpha}(0)h_0 s_0 + \sum_{\mathrm{b}_\ell\in\Phi_{\mathrm{mw}}/\mathrm{b}_0}\sqrt{\gamma_\ell}\bar{\alpha}(\theta_\ell)g_\ell s_\ell + v_0. \tag{4}$$

where the user subscript has been dropped from the azimuth angles θ_ℓ and the interfering channels g_ℓ since only a single user is served in each cell. The signal-to-interference-plus-noise ratio (SINR) in this case is thus given by

$$\mathsf{SINR}_0 = \frac{d_0^{-n}|h_0|^2\bar{\alpha}^2(0)}{I_{d_0} + Q_{\mathrm{N}}}, \tag{5}$$

where $I_{d_0} = \sum_{\mathrm{b}_\ell\in\Phi_{\mathrm{b}}/\mathrm{b}_0} d_\ell^{-n}|g_\ell|^2\bar{\alpha}^2(\theta_\ell)$ is the aggregate interference at u_0 and $Q_{\mathrm{N}} = \frac{\sigma^2 \mathrm{PL}_{\mathrm{ref}}}{P_{\mathrm{t,mw}} d_{\mathrm{ref}}^n}$ is the inverse signal-to-noise ratio at a given distance d_{ref} from the base station.

In this paper, we compute and compare the probability of coverage, which is given by

$$p_c(\lambda_{\mathrm{mw}}, n, T) = \mathbb{P}\left[\mathsf{SINR}_0 \geq T\right]. \tag{6}$$

The probability of coverage is the probability that a randomly chosen user in the cell has an instantaneous SINR greater than some target T.

Lemma 1:

$$p_c(\lambda_{\mathrm{mw}}, n, T) = \int_0^\infty f_{d_0}(d_0)\int_{-\infty}^{\infty} e^{-2\pi j\frac{Td_0^n}{Q_{\mathrm{N}}}s} \times \mathcal{L}_{I_{d_0}}\left(2j\pi d_0^n T s\right)\frac{\mathcal{L}_h(-2j\pi s)-1}{2j\pi s}\mathrm{d}s\mathrm{d}r \tag{7}$$

where the probability density function (pdf) of d_0, $f_{d_0}(r) = 2\pi\lambda_{\mathrm{mw}} r\exp(-\pi\lambda_{\mathrm{mw}}r^2)$, follows from the null probability of the 2-D Poisson point process Φ_{mw} [15].

The Laplace transform of the interference I_{d_0} is given by

$$\mathcal{L}_{I_{d_0}}(s) = \exp\left(-\lambda_{\mathrm{mw}}\int_{-\pi}^{\pi} d_0^{2-n}\, s\, \bar{\alpha}^2(\theta) \times {}_2\mathrm{F}_1\left(1, 1-\frac{2}{n}, 2-\frac{2}{n}, -d_0^{-n}s\right)\right). \tag{8}$$

The Laplace transform of the desired signal is

$$L_h(s) = \frac{1}{\left(1+\frac{s}{m_0}\right)^{m_0}}.$$

Proof: $p_c(\cdot)$ follows from [16] for a Poisson network with general fading distribution. $p_c(\cdot)$ is the complementary cumulative density function (CCDF) of SINR_0 when the desired signal power $|h_0|^2\bar{\alpha}^2(0)$ with $\bar{\alpha}^2(0) = 1$ is Gamma-distributed with PDF $p_h(h) = \frac{m_0^{m_0}h^{m_0-1}}{\Gamma(m_0)}\exp(-m_0 h)$. The interference I_{d_0} is the cumulative interference from all the base stations in the network, located at a distances $r_\ell > d_0, \forall \ell \neq 0$ from the typical user u_0. The distribution of the interfering signal powers $|g_\ell|^2\bar{\alpha}^2(\theta)$ can be calculated by leveraging the knowledge that $|g_\ell|^2$ is Chi-squared distributed with two degrees of freedom, θ is uniformly distributed on $[-\pi, \pi]$, and the structure of $\bar{\alpha}^2(\theta)$ given in (2). ■

The probability of coverage increases with m_0, since as the probability of a deep channel fade decreases for larger m_0; recall that a value of m_0 = 1 corresponds to a Rayleigh fading channel, while $m_0 \to \infty$, corresponds to a deterministic line-of-sight channel. The probability of coverage increases as the transmit power $P_{\mathrm{t,mw}}$ increases. Further, the probability of coverage increase with decreasing half-power beamwidth, $\theta_{3\mathrm{dB}}$, since sharper beams help in reducing interference.

$$\mathsf{SINR}_0 = \frac{d_0^{-n}|h_0|^2\bar{\alpha}^2(0)}{d_0^{-n}\sum_{k=1}^{K-1}|h_{0,k}|^2\bar{\alpha}^2(\theta_{0,k}) + \sum_{\mathrm{b}_\ell\in\Pi_{\mathrm{b}}/\mathrm{b}_0} r_\ell^{-n}\sum_{k=0}^{K-1}|g_{\ell,k}|^2\bar{\alpha}^2(\theta_{\ell,k}) + \frac{\sigma^2}{\frac{P_{\mathrm{t,mw}}}{PL_{\mathrm{ref}}}d_{\mathrm{ref}}^n}K}$$

$$= \frac{d_0^{-n}|h_0|^2\bar{\alpha}^2(0)}{d_0^{-n}I_{\mathrm{intra}} + \sum\limits_{\mathrm{b}_\ell\in\Phi_{\mathrm{mw}}/\mathrm{b}_0} r_\ell^{-n}g_\ell + \frac{\sigma^2}{\frac{P_{\mathrm{t,mw}}}{\mathrm{PL}_{\mathrm{ref}}}d_{\mathrm{ref}}^n}K} = \frac{d_0^{-n}S}{d_0^{-n}I_{\mathrm{intra}} + I_{d_0,\mathrm{mu}} + \frac{\sigma^2}{\frac{P_{\mathrm{t,mw}}}{\mathrm{PL}_{\mathrm{ref}}}d_{\mathrm{ref}}^n}K}. \quad (9)$$

IV. Performance Analysis for Multi-User Systems

In this section, we derive the probability of coverage for a typical user u_0, for multi-user beamsteering at the base stations. The SINR at u_0 follows from the received signal y_0 in (3), and is given in (9).

The signal $S = |h_0|^2\bar{\alpha}_0^2(0)$ is Gamma-distributed, $S \sim \Gamma[m_0, 1/m_0]$, similarly to the single-user case. The intra-cell interference $I_{\mathrm{intra}} = \sum_{k=1}^{K-1}|h_{0,k}|^2\bar{\alpha}^2(\theta_{0,k})$ is a function of K and the radiation pattern $\bar{\alpha}^2(\theta)$. Its Laplace transform in the example case of $\theta_1 = 0$ and $\theta_2 = 2\theta_{3\mathrm{dB}}$, is given by

$$\mathcal{L}_{I_{\mathrm{intra}}}(s) = \left(\frac{\theta-1}{\theta(1+s/d_0^n)\mathrm{FBR}} + \frac{\log(1+\frac{s}{d_0^\alpha})}{\theta s d_0^{-\alpha}}\right)^{K-1}. \quad (10)$$

Lemma 2: The probability of coverage $p_c(\lambda_{\mathrm{mw}}, n, T, K)$ for multi-user mmWave transmission is given by

$$p_c(\lambda_{\mathrm{mw}}, n, K, T) = \int_0^\infty f_{d_0}(d_0)\int_{-\infty}^{\infty} e^{-2\pi j\frac{TKd_0^n}{\mathrm{Q_N}}s}\times$$
$$\mathcal{L}_{I_{\mathrm{intra}}}(2j\pi d_0^n Ts)\,\mathcal{L}_{I_{d_0,\mathrm{mu}}}(2j\pi d_0^n Ts)\,\frac{\mathcal{L}_h(-2j\pi s)-1}{2j\pi s}\mathrm{d}s\mathrm{d}d_0, \quad (11)$$

where $f_{d_0}(d_0)$, $\mathrm{Q_N}$ and $\mathcal{L}_h(s)$ are defined as in the single-user case.

The Laplace transform of $I_{d_0,\mathrm{mu}}$ is a function of K and the radiation pattern $\bar{\alpha}^2(\theta)$ and is given by

$$\mathcal{L}_{I_{d_0,\mathrm{mu}}}(s) = \exp\left(-2\pi\lambda_{\mathrm{mw}}\int_{d_0}^\infty r(1-\mathcal{L}_p(s\,r^{-n}))\mathrm{d}r\right)$$

where

$$\mathcal{L}_p(s) = \left(\frac{\theta-1}{\theta(1+s/d_0^n)\mathrm{FBR}} + \frac{\log(1+\frac{s}{d_0^n})}{\theta s d_0^{-n}}\right)^K. \quad (12)$$

For the case of multi-user transmission, the probability of coverage decreases with the number of users K, and the half-power beamwidth $\theta_{3\mathrm{dB}}$. It increases with m_0, and the transmit power $P_{\mathrm{t,mw}}$. With more sophisticated beamforming or user scheduling, the per-user coverage probability is expected to increase.

V. Simulation Results and Discussion

In this section, we compare the performance of mmWave systems with that of microwave systems. The pathloss exponent is set to $n = 4$ for both mmWave and microwave systems. This choice is both tractable and in line with the measurement results of [6] that report a mmWave pathloss exponent of 3.86. The Nakagami parameter is set to $m_0 = 3$, and the number of antennas at the microwave base stations is either 4 or 8. The front-to-back ratio is given by $\mathrm{FBR} = -18$ dB in accordance with the Kathrein 742215 antenna model. The reference SNR is set to $Q_{\mathrm{N}} = 12$ dB.

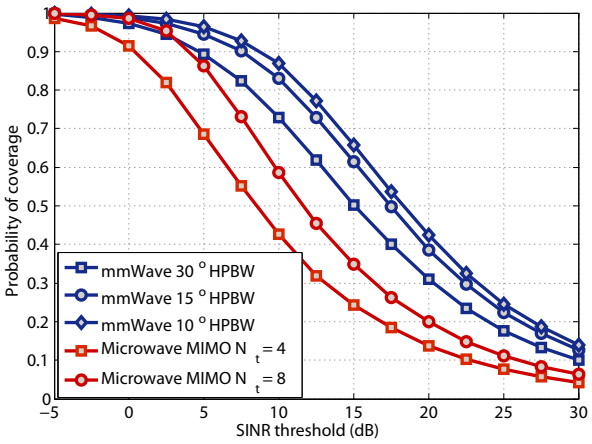

Fig. 1. The probability of coverage for single-user mmWave and microwave transmissions for $m_0 = 3$, $n = 4$, average SNR = 12 dB.

Figure 1 plots coverage probability for single-user mmWave systems for increasing SINR threshold, $T \in [-5,\ 30]$ dB and two different values for the half-power beamwidth $\theta_{3\mathrm{dB}} = 15, 30$ degrees. Figure 1 also shows the coverage performance of a microwave system with $N_{\mathrm{t}} = 4, 8$. Figure 1 shows that mmWave transmission has better coverage than microwave MIMO transmission for the same SINR threshold. As the half-power beamwidth decreases, the total interference power decreases resulting in improved coverage. The use of a Nakagami-m_0 distribution to account for the higher probability of line-of-sight paths in mmWave systems results in a steeper decaying coverage curve with a smaller tail when compared with microwave systems.

Figure 2 plots the coverage performance for multi-user transmission with $K = 2$ and $K = 3$ users. Figure 2 shows that the intra-cell interference in the mmWave systems, due to the overlapping beams, degrades the coverage performance of mmWave. For a half-power beamwidth of $\theta_{3\mathrm{dB}} = 30$ degrees, the mmWave coverage is comparable to microwave

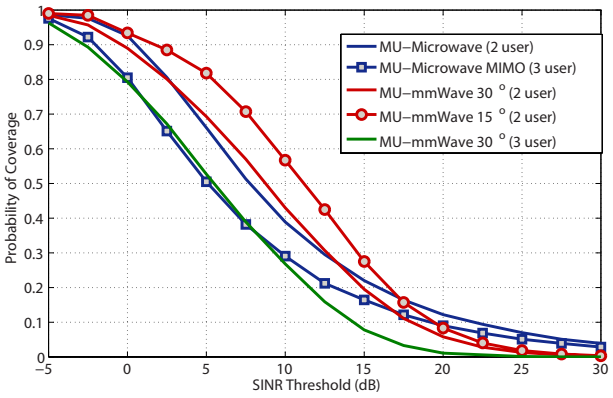

Fig. 2. The probability of coverage for multi-user mmWave and microwave transmissions for $m_0 = 3$, $N_\mathrm{t} = 8$, $n = 4$, average SNR = 12 dB, and K is either 2 or 3 users.

TABLE I
AVERAGE PER-USER RATE COMPARISON FOR MMWAVE AND MICROWAVE

	Microwave	MmWave
Single-user	92 Mbps	5.4 Gbps
Multi-user	72 Mbps	3.2 Gbps

transmission. As the half-power beamwidth decreases, however, the coverage of the mmWave system improves and becomes better than that of microwave system with $N_\mathrm{t} = 8$ antennas. Because as radiation patterns becomes narrower, beam overlap is reduced which ultimately reduces both intra-cell and inter-cell interference. Furthermore, the coverage probability decreases as the number of users increases and beamwidth is kept fixed.

The comparison in Figs. 1 and 2 showed comparable coverage performance for mmWave and microwave systems. This implies that both systems achieve comparable spectral efficiency. Since the bandwidth available for mmWave is much higher than the bandwidth available for current cellular systems transmissions (1 GHz of bandwidth instead of 20 MHz [1], [5]), the average rate per-user is expected to be significantly higher in mmWave systems. Table I presents a comparison of average per-user rates for single-user and multi-user ($K = 2$) transmissions. For this result, we assume that $m_0 = 3$, $N_\mathrm{t} = 8$, $\theta_{3\mathrm{dB}} = 30^o$, a 20 MHz microwave bandwidth, and a 1 GHz mmWave bandwidth. The average rates τ are obtained from the probability of coverage analysis,

$$\begin{aligned} \tau &= \mathbb{E}\left\{\log_2\left(1+\mathsf{SINR}_0\right)\right\} \\ &= \int_0^\infty \frac{\mathbb{P}\left[\mathsf{SINR}_0 > e^t - 1\right]}{\log(2)} dt. \end{aligned} \tag{13}$$

Table I shows a 50 times increase in the average rate for mmWave systems as compared to microwave systems.

VI. CONCLUSION

In this paper, we characterized the probability of coverage of large mmWave cellular networks serving single or multiple users per cell, comparing with typical microwave systems. We found that coverage between the two systems was comparable, thus the larger bandwidths at mmWave frequencies can support much higher data rates than microwave systems. We expect further improvements with more sophisticated beamforming techniques for mmWave systems. Further work is needed to evaluate performance in more realistic propagation settings including blockage effects.

REFERENCES

[1] A. Ghosh, R. Ratasuk, B. Mondal, N. Mangalvedhe, and T. Thomas, "LTE-advanced: next-generation wireless broadband technology," *IEEE Wireless Commun. Mag.*, vol. 17, no. 3, pp. 10–22, 2010.

[2] A. Damnjanovic, J. Montojo, Y. Wei, T. Ji, T. Luo, M. Vajapeyam, T. Yoo, O. Song, and D. Malladi, "A survey on 3GPP heterogeneous networks," *IEEE Wireless Commun. Mag.*, vol. 18, no. 3, pp. 10–21, 2011.

[3] R. Daniels and R. W. Heath, Jr., "60 GHz wireless communications: emerging requirements and design recommendations," *IEEE Veh. Technol. Mag.*, vol. 2, no. 3, pp. 41–50, 2007.

[4] C. Doan, S. Emami, A. Niknejad, and R. Brodersen, "Millimeter-wave cmos design," *IEEE J. Solid-State Circuits*, vol. 40, no. 1, pp. 144–155, 2005.

[5] Z. Pi and F. Khan, "An introduction to millimeter-wave mobile broadband systems," *IEEE Commun. Mag.*, vol. 49, no. 6, pp. 101–107, 2011.

[6] T. Rappaport, Y. Qiao, J. Tamir, J. Murdock, and E. Ben-Dor, "Cellular broadband millimeter wave propagation and angle of arrival for adaptive beam steering systems," in *proc. of IEEE Radio Wireless Symp.*, 2012, pp. 151–154.

[7] J. Murdock, E. Ben-Dor, Y. Qiao, J. Tamir, and T. Rappaport, "A 38 GHz cellular outage study for an urban outdoor campus environment," in *proc. of IEEE Wireless Commun. and Networking Conf.*, 2012, pp. 3085–3090.

[8] S. Rajagopal, S. Abu-Surra, Z. Pi, and F. Khan, "Antenna array design for multi-gbps mmwave mobile broadband communication," in *proc. of IEEE Global Telecom. Conf.*, 2011, pp. 1–6.

[9] A. Sayeed and N. Behdad, "Continuous aperture phased MIMO: Basic theory and applications," in *proc. of Allerton Conf. on Commun., Control, and Computing*, Oct. 2010, pp. 1196 –1203.

[10] J. Nsenga, A. Bourdoux, and F. Horlin, "Mixed analog/digital beamforming for 60 GHz MIMO frequency selective channels," in *proc. of IEEE Int. Conf. on Commun.* IEEE, pp. 1–6.

[11] X. Zhang, A. Molisch, and S.-Y. Kung, "Variable-phase-shift-based RF-baseband codesign for MIMO antenna selection," *IEEE Trans. Signal Process.*, vol. 53, no. 11, pp. 4091–4103, Nov. 2005.

[12] Z. Pi, "Optimal transmitter beamforming with per-antenna power constraints," in *proc. of IEEE Int. Conf. on Commun.*, Jun. 2012, pp. 1–5.

[13] O. El Ayach, R. W. Heath, Jr., S. Abu-Surra, S. Rajagopal, and Z. Pi, "Low Complexity Precoding for Large Millimeter Wave MIMO Systems," in *proc. of IEEE Int. Conf. on Commun.*, Jun. 2012, pp. 1–6.

[14] S. Singh, R. Mudumbai, and U. Madhow, "Interference analysis for highly directional 60 GHz mesh networks: the case for rethinking medium access control," *IEEE/ACM Trans. Netw.*, vol. 19, no. 5, pp. 1513–1527, 2011.

[15] J. G. Andrews, F. Baccelli, and R. Krishna Ganti, "A tractable approach to coverage and rate in cellular networks," *IEEE Trans. Commun.*, vol. 59, no. 11, pp. 3122–3134, Nov. 2011.

[16] F. Baccelli, B. Blaszczyszyn, and P. Muhlethater, "Stochastic analysis of spatial and opportunistic Aloha," *IEEE J. Sel. Areas Commun.*, vol. 27, no. 7, pp. 1105–1119, sept. 2009.

[17] F. Baccelli and B. Blaszczyszyn, *Stochastic geometry and wireless networks. Volume II: applications*. NOW publishers, 2009.

[18] T. Bai, R. Vaze, and Heath, "Using random shape theory to model blockage in random cellular networks," in *proc. of Intl. Conf. on Signal Proc. and Comm.*, Jul. 2012, pp. 1–5.